

MODE SPLITTING IN A SPHERICAL MICROCAVITY UNDER RADIATION PRESSURE

K.I. Rusakov¹, A.A. Gladyshchuk¹, S.V. Chugunov¹, Y. P. Rakovich^{1,2},
M. Gerlach², J.F. Donegan²

¹ Brest State Technical University, Brest

² School of Physics, Centre for Research on Adaptive Nanostructures and Nanodevices, Trinity College Dublin, Dublin

In recent years the radiation pressure created by a focused laser beam can be used to trap, levitate and manipulate micro- or nanometer-sized dielectric particles and biological cells [1-2]. Although photons are massless particles, they can transfer their momentum to the particle. The strong gradient of the electro-magnetic field intensity in the region of the beam waist gives rise to the so-called gradient force, which when working against the gravitational force provides a method for optical binding and manipulation of ultra-fine particles and mesoscopic systems. In addition, a beam of light can exert sufficient radiation pressure to move a microstructured object along the direction of the beam propagation under the effect of the scattering force. This radiation-pressure-induced opto-mechanical interaction shows great promise for a variety of applications in the field of optically actuated micro-optical-electromechanical systems (MOEMS) [3-4], laser cooling [5], spectrum analysis [6], optical information processing [4,6] and quantum informatics [5]. We present new results on the mode manipulation by radiation pressure in a micro-scale optical cavity with a thin shell. The light coupled into a spherical microcavity is trapped inside the microsphere near the circumference by total internal reflection, causing the morphology dependent resonances, also called whispering gallery modes (WGMs). In our approach, we utilise small spherical microcavity structures ($< 5 \mu\text{m}$ diameter) whose modes are highly sensitive to changes of the refractive index of the sphere itself [7-8] or to the environment in close proximity to the sphere surface [9-10]. In the latter case, the sensitivity is due to the evanescent field of the WGMs, which extend into the surrounding medium. Along with these properties, WGMs show remarkable sensitivity to deformation which allows fine tuning of the WGM's spectral position and Q-factor [11,12]. Motivated by recent studies of the elastic properties of polyelectrolyte (PE) multilayer [13], we applied a layer-by-layer (LbL) deposition approach to fabricate a thin PE elastic shell on the surface of melamine formaldehyde (MF) microspheres. Varying the number of oppositely charged polyelectrolyte bi-layers deposited on MF templates provided the variation in the shell thickness. The value of Young's modulus of PE LbL films (100–200 MPa) falls in the range characteristic for highly cross-

linked rubber [14]. Efficient coupling of the quantum dot (QD) emission with the WGM of the microsphere was achieved by coating the spheres with one monolayer of CdTe semiconductor nanocrystals on top of the PE multiplayer [15]. The photoluminescence from these quantum dots is size dependent, which allows the tuning of the excitation maximum over a wide spectral range. In our approach the trapping of the microsphere in an optical tweezing setup was achieved with a tightly focused cw laser beam when the MF/PE/CdTe microsphere-emitter was placed on a glass substrate. Due to a strong difference in elastic properties of MF and the PE multilayer film [13], the radiation-pressure-induced deformation of the PE shell is the crucial factor controlling the WGM structure in the micro-PL spectra of the microcavity. The PE shell deformability was increased through contact of the shell with a salt-containing solution, which changes the mechanical properties of the PE multilayer. We have chosen spheres with a diameter of 3 μm for our experiments. These spheres possess a large free spectral range between resonant WGM peaks that allows accurate identification of the polarisation and mode number of WGMs. The mode linewidth or quality factor Q are relatively unaltered by effects such as absorption by the CdTe QD monolayer [16]. We investigated the possibility of controlling the splitting of the WGM resonances in the microsphere/QDs system by radiation pressure. The experimental approach presented here should lay the groundwork for application of WGMs in spherical microcavities with an elastic shell for photonic applications.

The samples were made of commercially available MF microspheres with a specific diameter of 3.078 μm (Particle Size Standard, Micro Particles GmbH, Berlin, Germany). The optically transparent sphere is first coated with several PE layers. Based on electrostatic interaction, the layers were assembled on the sphere surface in a LbL technique described elsewhere [17]. The MF microsphere is slightly positively charged with negatively charged poly(styrene sulfonate) (PSS) and positively charged poly(allylamine hydrochloride) (PAH) used to build the alternating layers. One bi-layer consists of a pair of one PSS and one PAH layer. The average thickness of one PE layer is approximately 1.5 nm [18]. The PE multilayer forms a soft shell around the more rigid MF microsphere core. We prepared samples with up to 10 bi-layers. In the final step, one monolayer of CdTe QDs is applied on top of the PE multilayer shell. The QDs are negatively charged due to the thioglycolic acid stabilizer on the QDs surface, they are synthesized in an aqueous solution as described in [19]. The outermost layer on the sphere must be the positively charged PAH to allow the QDs to be bonded to the surface, also due to an electrostatic force. The CdTe forms a closed packed dense monolayer of QDs on the sphere surface. In order to control the elasticity of the PE shell, we used an additional

chemical procedure to modify the mechanical properties of the PE layer on the surface of some of the samples. Before these spheres were coated with a QD monolayer, we kept them for 5 days in a highly concentrated NaCl (7 Mol/l) solution as discussed in [14]. This treatment reduces the solidity of the PE layer resulting in a softer, more elastic layer. A xyz-microstage with a spatial resolution of 0.1 $\mu\text{m}/\text{step}$ allows an accurate focusing of the laser beam through the high NA (0.9) microscope objective (Leitz, Germany) at 100x magnification. The diameter of the focus was adjusted to be approximately 1.5 μm . The excitation source is an Ar^+ -ion laser ($\lambda = 514.5 \text{ nm}$, up to 45 mW power), coupled into the system. The PL signal was collected by the same objective, and filtered by notch and plasma filters. An air-cooled CCD camera was used as the detector.

The discrete wavelengths corresponding to the WGMs within a microsphere can be identified by the angular mode number l , which describes the angular variation of the internal mode intensity [20]. The radial variation in the internal field is described by the mode order n , which indicates the number of radial maxima in the distribution of the mode intensity. For each mode number and order there exists both a transverse electric TE mode having no radial electric field component, and a transverse magnetic TM mode with no radial magnetic field component. WGMs are also wavelength degenerate with respect to the azimuthal (m) modes due to the spherical symmetry of the microcavity. This means that orbits with various inclinations, described by various m -modes have the same pathlengths and consequently the same resonance wavelength. The total number of these m -modes, originating from a certain mode l , is governed by the distribution of electro-magnetic fields confined in the microsphere and in the approach of the normal mode concept is $2l + 1$. The so-called fundamental mode $m = l$ is situated in the equatorial plane, the smallest azimuthal mode $m = 0$ is located perpendicular to the fundamental mode in the polar region as indicated in Fig. 1.

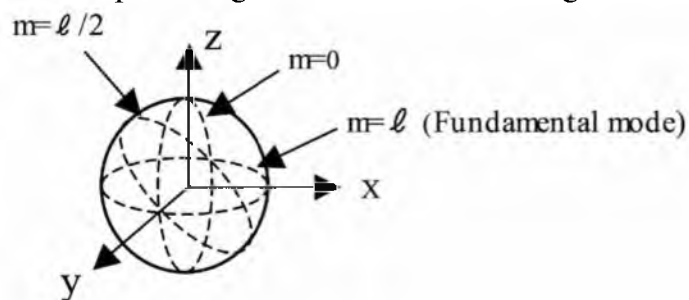


Fig. 1. Spatial orientation of the optical resonances with respect to the azimuthal mode number m .

One of the ways to reveal different m-modes is to deform the microsphere, for example, using a compression device [12] or as recently published by laser heating a polystyrene sphere in an ion trap [21]. Shape distortion breaks the azimuthal symmetry and results in a lifting of the degeneracy. In a deformed sphere, photonic orbits with various inclinations have different pathlengths and therefore, the spectral positions of m-modes are no longer the same. In other words, a single WGM peak in the spectrum of a perfect sphere is now split into a series of azimuthal resonances. The m-modes with “+” and “-” signs, designating clockwise and counter-clockwise rotations, still have the same resonance wavelength. As a result no degeneracy is removed between m and -m in the deformed microsphere and the new degeneracy of WGMs is now $\ell + 1$ with m progressing from 0 to ℓ . Perturbation theory provides an analytical expression for the frequency shifts and mode splitting of each of the WGMs for an oblate spheroid with a small amplitude of distortion $e = (\mathbf{r}_p - \mathbf{r}_e)/a \ll 1$, where the polar and equatorial radii are \mathbf{r}_p and \mathbf{r}_e , respectively [22].

$$\lambda_m(m, e) = \lambda_{\ell, n} \left\{ 1 + \frac{e}{6} \left[1 - \frac{3m^2}{\ell(\ell+1)} \right] \right\} \quad (1)$$

$\lambda_m(m, e)$ is the resonance wavelength of the azimuthal mode, which is dependent on the distortion and the m-mode number. $\lambda_{\ell, n}$ is the resonance wavelength for a perfect sphere of radius a. Increasing the deformation of the sphere leads to a stronger splitting and a higher free spectral range between the azimuthal modes, which increase quadratically with the mode number m. A physically cross-linked network of PE molecules forms an elastic LbL shell on the surface of MF microspheres. The strong difference in elastic properties of the MF core and the PE multilayer film suggests the possibility of revealing m-modes by deformation of the elastic surface shell. However, a controllable mechanical deformation of 3- μm microspheres combined with micro-PL spectroscopy is difficult to realize. The alternative is to use the radiation force acting on a microcavity on a substrate, illuminated by a tightly focused laser beam. In this optical trapping experimental scheme, radiation pressure is applied to the sphere. A downward radiation force is pressing the sphere onto the glass substrate. Instead of producing a deformation resulting in an oblate spheroid shape, we only apply radiation pressure which is strong enough to deform the soft PE multilayer on the sphere surface. The solid MF core is not distorted, as the radiation pressure is not sufficient to deform the whole sphere. Only the soft PE multilayer is compressed under radiation pressure between the solid substrate and the MF core. Total internal reflection within the microcavity system occurs at the boundary between the surrounding medium (air) and the soft PE multilayer. Therefore, a deformation of the PE

shell is affecting the resonance frequency of the modes. The primary condition for optical trapping is a high intensity gradient of a laser beam, in our case a Gaussian beam, obtained by an objective with high numerical aperture. The schematic setup is shown in Fig. 2.

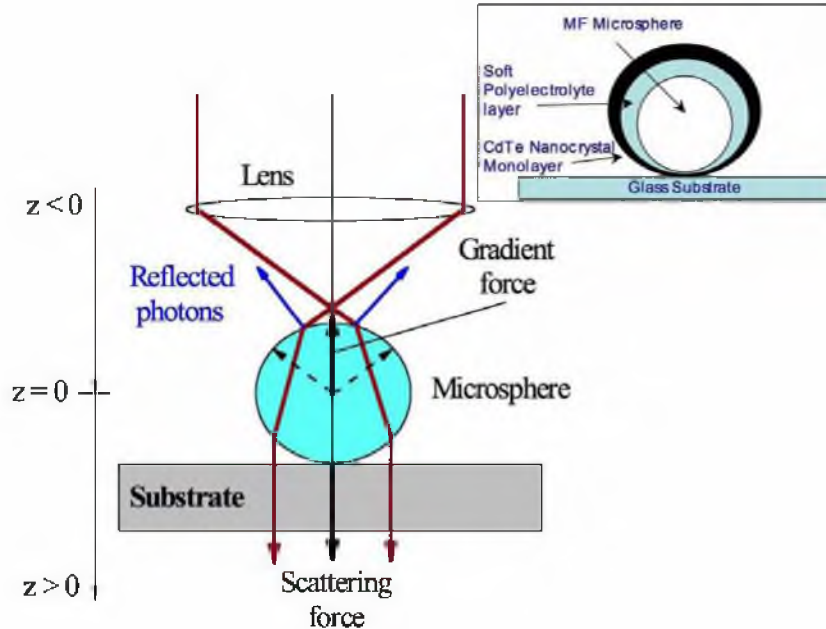


Fig. 2. The scheme for radiation force on a spherical microcavity. The inset shows the distortion of the spherical shape caused by the sphere pushed on the substrate.

We assume the origin of the reference Cartesian coordinate system to be in the centre of the sphere and z - and y -axes are normal and parallel to the substrate, respectively. The strong gradient of the electro-magnetic field intensity in the region of the beam waist gives rise to the so-called gradient force (Fig. 2). The net radiation force can either be in the direction of the beam or in opposite direction, depending on the position of the laser focus. The interplay of scattering and gradient forces provides a way of trapping the particle within the beam and manipulating it in all three dimensions. Both of these forces scale linearly with light intensity and when the gradient force dominates the scattering force, a restoring force with a magnitude of pico-newtons acts to confine the particle to the most intense region in the laser beam and a stable trap is created. The inset in Fig. 2 shows the non-uniform deformation of the soft PE multilayer under radiation pressure for the sphere placed on a solid substrate. For microcavity sizes larger than the wavelength of the laser irradiation, the net force exerted on the microsphere by a focused Gaussian beam can be calculated by the use of generalized Lorentz-Mie theory (GLMT) [23]. The GLMT can be used to calculate the spectrum of the scattered light for different positions of the particle in the beam and for

different types of incoming waves. In this approach, the radiation pressure exerted by the laser beam propagating toward the positive z direction and impinging on a spherical microparticle located along the axis of the beam is given by

$$F_{rad} = \frac{2P}{c\pi\omega_0^2} C_{pr} \quad (2)$$

where P is the power of the laser beam, ω_0 the spot size of the focused beam and C_{pr} the radiation pressure cross-section which is given by [23]

$$C_{pr} = \frac{\lambda^2}{2\pi} \sum_{n=1}^{\infty} \frac{2n+1}{n(n+1)} |g_n|^2 \text{Re}[a_n + b_n - 2a_n b_n^*] + \frac{n(n+2)}{n+1} \text{Re}[g_n g_{n+1}^* (a_n + b_n + a_{n+1}^* + b_{n+1}^* - 2a_n a_{n+1}^* - 2b_n b_{n+1}^*)] \quad (3)$$

In this equation, the beam shape coefficient g_n for an on-axis Gaussian beam is

$$g_n = \left(1 + i2s \frac{z_0}{\omega_0}\right)^{-1} \exp(ikz_0) \exp\left[\frac{-s^2(n-1)(n+2)}{1 + i2(s z_0 / \omega_0)}\right] \quad (4)$$

where s is defined by $s = 1/k\omega_0$, k is the wavenumber and z_0 is the coordinate of the beam-waist centre. The Mie-coefficients a_n and b_n are the scattering coefficients which were calculated with expressions based on the Lorenz-Mie theory [20]. Figure 3 shows the calculated radiation force F_{pr} for a variable focus position along the z-axis in the centre of the sphere with a diameter of 3.078 μm .

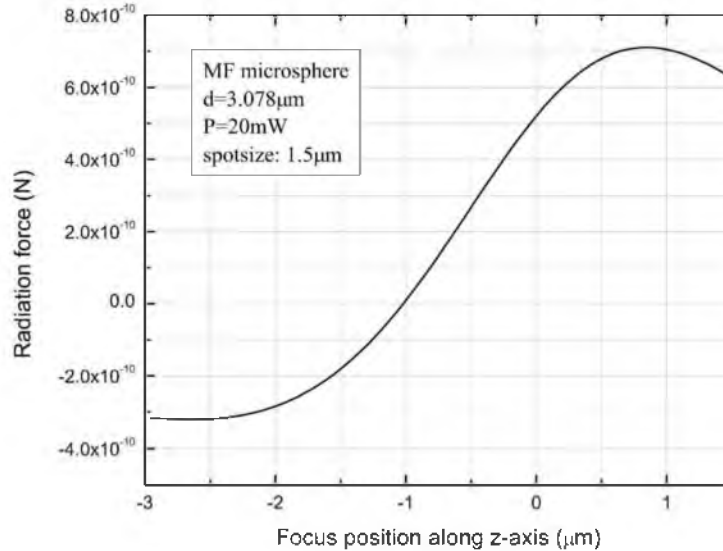


Fig. 3. Calculation of radiation pressure applied to a microsphere in the sphere centre along the z-axis of Fig. 2.

This occurs when the resulting gradient force exceeds the scattering force. A positive F_{pr} pushes the sphere downwards onto the solid substrate. The value $z = 0$ on the x-axis in Fig. 2 corresponds to the centre of the sphere. Positive z values are focus positions below the centre towards the substrate and negative values of z corresponds to a focus point above the sphere centre. A freely moving microsphere would be trapped at the point where the radiation force is zero, which is at $z = -1 \mu\text{m}$ in our calculations.

When a laser beam is focused at this point, the scattering force and the gradient force compensate each other. When the focus is moved further up, the resulting radiation force is pulling the sphere upwards and when the focus is moved further down, the sphere is pushed onto the substrate with the maximum radiation pressure at around $0.6 \mu\text{m}$ ($z = 0.9 \mu\text{m}$) above the substrate. The calculations clearly demonstrate the possibility of controlling the radiation pressure by tuning the focus position, implying a non-contact method of controllable tuning modification of WGMs in a spherical microcavity with a compressible surface shell. The PL spectra of single microspheres with 12 nm and 30 nm thick PE shells, respectively and one monolayer of CdTe QDs were taken at different focus positions and excitation power. In order to modify the stiffness of the PE shell, the sample with the 15 nm shell was kept for 5 days in a highly concentrated NaCl (7 Mol/l) solution, before these spheres were coated with the QD layer. This treatment reduced the solidity of the PE layer resulting in a softer surface layer.

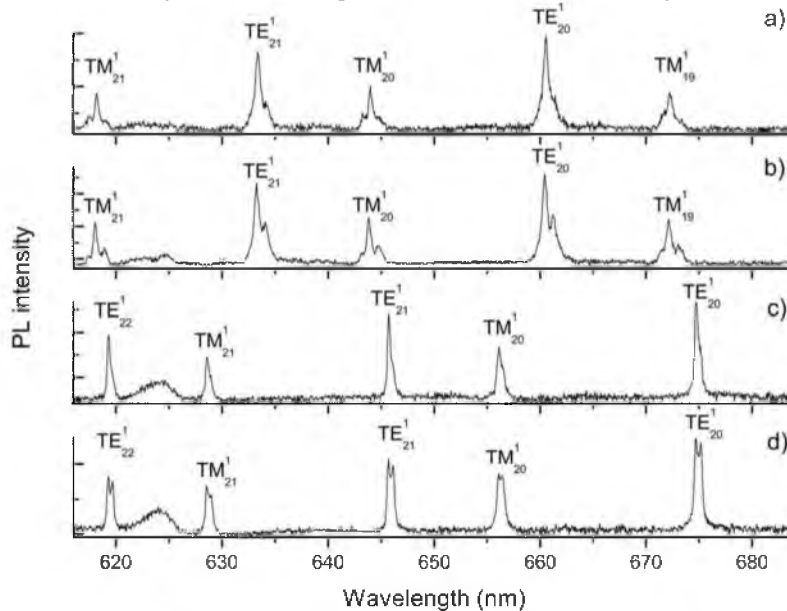


Fig. 4. PL spectra of microspheres while trapped in a cw laser beam under radiation pressure. **(a)** and **(b)** Same microsphere sample (4 bi-layers), excitation power $P = 15 \text{ mW}$ taken at different focus positions. **(c)** and **(d)** Another microsphere sample (5 bi-layers) modified with a salt solution and taken at considerably lower excitation power $P = 5 \text{ mW}$.

Figure 4 shows the spectra of four measurements. The focused laser beam applies a radiation force on a single microsphere as illustrated in Fig. 2. The laser also excites the QDs on the sphere surface. The spectra of a single sphere shown in Fig. 4(a) and 4(b) were taken with the micro-PL setup with a different focal position. The sphere is coated with 4 bi-layers of PE but not softened in a salt solution. In the first case (see Fig. 4(a)), the PL spectrum was recorded with a focus position of $z = -2.5 \mu\text{m}$, which is $1 \mu\text{m}$ above the microsphere. According to theoretical predictions (Fig. 3), the laser beam causes an upward radiation pressure exerted on the sphere. Thus, the stronger peaks in Fig. 4 were identified as TE modes, whereas the smaller peaks observed in the micro-PL spectra are TM modes. The TE and TM resonances were identified by angular mode number ℓ (subscript number) and the radial mode order n (superscript number) in the spectrum. The angular mode number is necessary to determine the spectral mode positions for each azimuthal mode individually (see Eq. 1). All peaks in the spectrum show some weak indication of splitting due to the radiation pressure and the weight of the sphere ($F_{\text{weight}} = 1.6 \times 10^{-12} \text{ N}$). When focused inside the sphere on the substrate ($z = -1.5 \mu\text{m}$) as shown in Fig. 4(b), a second peak which is slightly red-shifted with respect to the original mode is now clearly observed. The splitting of the WGM peak towards longer wavelength is in very good agreement with the theory, predicting that the deformation causes the lifting of the mode degeneracy and shifting the azimuthal modes to longer wavelengths.

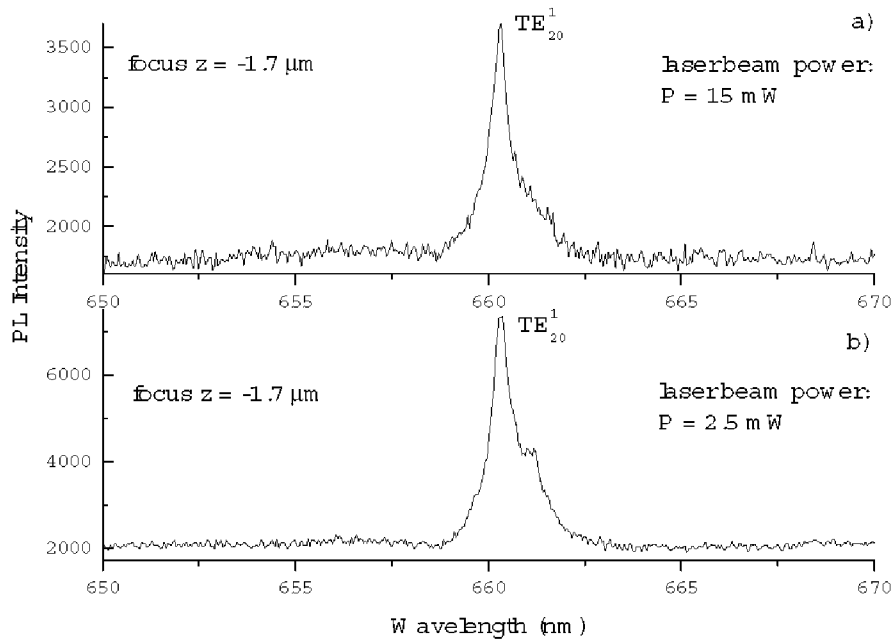


Fig. 5. Excitation of a single sphere at constant focus position $z = -1.7 \mu\text{m}$ at **(a)** $P = 15 \text{ mW}$ and **(b)** $P = 2.5 \text{ mW}$.

As a further demonstration of radiation pressure effect, we have studied the spectrum of a single sphere at a constant focal position $z = -1.7 \mu\text{m}$ for two different laser beam intensities (Fig. 5). The first spectrum was taken at $P = 15 \text{ mW}$ excitation power, the second one at $P = 2.5 \text{ mW}$. According to our calculations, the radiation force is directed upwards in the opposite direction of the laser beam at a focus position of $z = -1.7 \mu\text{m}$ (see Fig. 3). In these experimental conditions an increase in radiation power causes a decrease in splitting.

A mathematical model based on Eq. 5 can verify that the observed peak structure is indeed caused by lifting the azimuthal mode degeneracy. By means of this model, individual WGMs can be approximated by Lorentzian-shaped azimuthal peaks. In a perfectly spheroid deformation, the original peak would vanish and split into the azimuthal resonances (see Eq. 1). As our sample sphere experience a non-uniform distortion within the soft shell of the microcavity, we expanded the model for the azimuthal splitting. The modes with high mode number m , which travel around the circumference near the equator of the sphere, would be strongly red-shifted in a perfect oblate spheroid. Our samples experience no shape deformation near the equator and therefore, the modes located there are not red-shifted but instead they still have the original resonance frequency of a non-deformed sphere. To consider this fact, we included the Lorentzian peak of the original mode into the model, which is the first term in Eq. 5.

The second term is the sum of all azimuthal Lorentzian peaks in a deformed oblate spheroid. We assume that there is still a strong resonance at the original resonance frequency as a result of the non-uniform deformation overlapped by the split azimuthal modes

$$F(\lambda) = \frac{I_0 \cdot \Delta\lambda_{FWHM}}{(\lambda - \lambda_0) \left(\frac{1}{2} \Delta\lambda_{FWHM} \right)^2} + \sum_{m=0}^l \frac{I \cdot \Delta\lambda_{FWHM}}{(\lambda - \lambda_m) \left(\frac{1}{2} \Delta\lambda_{FWHM} \right)^2}. \quad (5)$$

The first term in the equation is the original resonance of the undistorted sphere, the second term is the sum of all azimuthal peaks. I and I_0 are the intensities of the Lorentzian peaks. The linewidth of the resonances which is determined to be $\Delta\lambda = 0.3 \text{ nm}$ ($Q \approx 2200$) and the original resonance wavelength λ_0 are taken from the measured spectrum to model the WGM lineshape. The shape of the modelled peak is fitted to the measured peak by changing the ellipticity e of the microsphere/PE multilayer structure.

The effect of radiation pressure on the WGM lineshape was found to be even more pronounced for the MF microsphere with 5 bi-layers of PE (Fig. 4(c) and 4(d)). The laser output power in this measurement was 5 mW . The

graph in Fig. 4(d) clearly shows the splitting of the TE modes into two peaks with almost equal intensities. The spheres for this experiment were treated with NaCl solution for increased softening of the PE layer. As a result, the splitting was achieved at lower excitation power with only 1/3 of the power used in the case of the 4 bi-layer spheres (Fig. 4(a) and 4(b)), which were not treated with the NaCl solution. The softening allows us to excite the samples with lower laser intensity to avoid thermal damage and photodegradation of the CdTe QDs. Applying the same simulation procedure for a peak of the spectrum in Fig. 4(d) the ellipticity was determined to be $e = 5.0 \cdot 10^{-3}$.

1. *Ashkin A.* // IEEE J. Quantum Electron. 2000. №.6, P. 841-856.
2. *Molloy J. E., Padgett M. J.* // Contemp. Phys. 2002. V. 43, P. 241-258.
3. *Gauthier R. C., Tait R. N., Mende H.* // Appl. Opt. 2001. V. 40, P. 930-936.
4. *Sulfridge M., Saif T., Miller N. et. al.* // J. Microelectromech. Syst. 2002. V.11, p. 574-580.
5. *Höhberger Metzger C., Karrai K.* // Nature. 2004. V. 432, P. 1002-1009.
6. *Dragoman D., Dragoman M.* // Applied Optics. 1999. V. 38, P. 6773-6779.
7. *Teraoka I., Arnold S.* // J. Opt. Soc. Am. B. 2006. V. 23, P. 1434-1441.
8. *Teraoka I., Arnold S.* // J. Opt. Soc. Am. B. 2006. V. 23, P. 1381-1389.
9. *Arnold S., Khoshsima M., Teraoka I. et. al.* // Opt. Lett. 2003. V. 28, P. 272-274.
10. *Teraoka I., Arnold S., Vollmer F.* // J. Opt. Soc. Am. B. 2003. V. 20, P. 1937-1946.
11. *Tzeng H.-M., Long M. B., Chang R. K., Barber P. W.* // Opt. Lett. 1985. V. 10, P. 209-211.
12. *Ilchenko V. S., Volikov P. S., Velichansky V. L. et. al.* // Opt. Commun. 1998. V.145, P. 86-90.
13. *Lulevich V. V., Andrienko D., Vinogradova O. I.* // J. Chem. Phys. 2004. V. 120, P. 3822-3826.
14. *Lebedeva O. V., Kim B.-S., Vasilev K., Vinogradova O. I.* // J. Colloid Interface Sci. 2005. V. 284, P. 455-462.
15. *Rakovich Y.P., Yang L., McCabe E. M. et. al.* // Semicond. Sci. Technol. 2003. V.18, P. 914-918, 2003.
16. *Rakovich Y. P., Donegan J. F., Gerlach M. et. al.* // Phys. Rev. A. 2004. V.70, P. 051801-1-051801-4.
17. *Susha A. S., Caruso F., Rogach A. L. et. al.* // Coll. Surf. A. 2000. V.163, P. 39-44.
18. *Komarala V. K., Rakovich Y. P., Bradley A. L. et. al.* // Nanotechnology. 2006. V. 17, P. 4117-4122.
19. *Gaponik N., Talapin D. V., Rogach A. L. et. al.* // J. Phys. Chem. B. 2002. V. 106, P. 7177-7185.
20. *Chang R.K., Campillo A.J.* Optical Processes in Microcavities. NY.: World Scientific Pub Co Inc, 1996. 452 p.
21. *Trevitt A.J., Wearne P.J.* // Opt. Lett. 2006. V. 31, P. 2211-2213.
22. *Lai H.M., Leung P.T., Young K. et. al.* // Phys. Rev. A. 1990. V. 41, P. 5187-5198.
23. *Ren K.F., Grehan G., Gouesbet G.* // Appl. Opt. 1996. V. 35, P. 2702-2710.